Available online at www.sciencedirect.com
SCIENCE DIRECT®
Journal of Sound and Vibration 281 (2005) 171–187
JOURNAL OF SOUND AND VIBRATION
www.elsevier.com/locate/jsvi

Theoretical/empirical prediction and measurement of the sound produced by vortex pairing in a low Mach number jet

C. Schram[a,1], S. Taubitz[a,2], J. Anthoine[a,*], A. Hirschberg[b]

[a]*von Karman Institute for Fluid Dynamics, Chaussee de Waterloo 72, 1640 Rhode-st-Genese, Belgium*
[b]*Technische Universiteit Eindhoven, Eindhoven, Netherlands*

Received 8 October 2003; accepted 12 January 2004
Available online 29 September 2004

Abstract

The sound produced by vortex pairing in a Mach 0.1, acoustically excited air jet is considered. The sound produced by vortex pairing is predicted on the basis of an experimental description of the flow field and using an aeroacoustical analogy. The experimental data is provided by particle image velocimetry. The aeroacoustical analogy is a conservative formulation of the vortex sound theory that has been developed in a previous work. This formulation has been shown to be robust when the flow data contains approximations or experimental uncertainties, as is the case here. The prediction is compared to measurements of the sound produced by the excited jet. The spectrum exhibits frequency components that are associated to the pairing, an intermittent second pairing, and the acoustical excitation. The agreement between the sound prediction and the acoustical measurements is good for the first two harmonics related to the first pairing. This demonstrates that the authors' conservative formulation of the vortex sound theory allows a correct sound prediction in spite of the uncertainties on the flow data.

*Corresponding author. Tel.: +32 2 359 9615; fax: +32 2 359 9600.
E-mail address: anthoine@vki.ac.be (J. Anthoine).
[1]Also at LMS International, CAE Division, Leuven, Belgium.
[2]Also at Mechanical and Industrial Engineering Department, University of Illinois at Chicago, 842 West Taylor Street, Chicago, IL 60607, USA.

0022-460X/$ - see front matter © 2004 Elsevier Ltd. All rights reserved.
doi:10.1016/j.jsv.2004.01.031

1. Introduction

It is generally agreed that the beginning of modern aeroacoustics coincides with the publication of the aeroacoustic analogy of Lighthill [1,2]. The idea of rearranging the Navier–Stokes equations in a form resembling the inhomogeneous wave equation, combined with the identification of the resulting source term with a modal expansion made of monopoles, dipoles and quadrupoles, has indeed given an unprecedented insight into aerodynamic sound-producing mechanisms.

Aeroacoustical analogies are also quite powerful to obtain a meaningful prediction of aerodynamically generated sound in spite of scarce or inaccurate flow data. The purpose of this work is to predict the noise produced by vortex pairing on the basis of experimental data. The vortex pairing occurs in a low Mach number excited jet, and is measured by means of particle image velocimetry. So far, the sound produced by a vortex interaction such as vortex pairing has only been predicted on the basis of theoretical models or numerical predictions.

The most thorough experimental study of vortex pairing sound has been performed by Bridges [3] in his thesis work. He measured the directivity of the sound emitted by vortex pairing in a forced jet, and reported an excellent agreement with the theoretical quadrupolar directivity that is expected from the theory. Bridges and Hussain [4] remarked however that the directivity of the sound produced by vortex rings in a circular jet does not depend on the details of their interaction. Their evolution just needs to be axisymmetric [5]. Conversely, the temporal evolution and amplitude of the acoustical emission is very sensitive to details in the flow field. Ryu and Lee [6] stressed the need for a detailed description of the vortex motion that is imposed by the successive time derivatives that are involved in the aeroacoustical analogy. Quoting Bridges and Hussain [4]: "It is also important to note that one cannot use the experimental vorticity data to calculate sound pressure directly. The small, but unavoidable, experimental error [...] will dominate the result." More specifically, they identified the fundamental reason why the use of experimental data to calculate directly the sound production is problematic: the non-conservation of integrals of motion that is due to experimental errors [7,4]. This appeared indeed to be a key issue in this work.

To predict the sound produced by vortex pairing, a formulation of the aeroacoustic analogy known as vortex sound theory is used. Vortex sound theory is an alternative version of Lighthill's analogy in which the acoustical source is expressed as a function of the vorticity field. This makes this formalism very powerful for the prediction of the sound generated by localized vortex interactions, because the non-vanishing vorticity field is in such cases much more confined in space than the corresponding velocity field. This renders the integration of the acoustical source term considerably simpler than applying Lighthill's analogy.

Another advantage of vortex sound theory, mostly unnoticed in the literature, is that this analogy offers a powerful formalism to compensate for inaccuracies in the flow model. This allowed Möhring [8] to obtain a meaningful prediction of the sound produced by a very crude two-dimensional vortex filament pairing model. Although put quite implicitly in this paper, such a result is quite spectacular if one considers that vortex stretching—which plays a significant role in the reciprocal impulse exchange generating sound in that case—was not accounted for by the flow model. This has triggered many ideas developed by Schram and co-workers in previous papers leading to the derivation of a so-called conservative formulation of the vortex sound theory [9,10].

Kambe and Minota [11] used a more realistic axisymmetric vortex blob model to obtain a sound prediction that exhibits the essential features of a realistic vortex pairing sound generation.

Yet, the effect of core deformation was not accounted for. Shariff et al. [12] incorporated into the model used by Kambe and Minota [11] the possibility for the vortex cores to be strained into ellipses. The result was the addition of a high-frequency noise component due to the nutation of the vortex cores to the low-frequency component associated with the leapfrogging period.

Going further in complexity, Tang and Ko [13] used the method of contour dynamics to calculate the evolution of the vortex rings. This inviscid method permits a continuous deformation of the contour of the vortex blobs, and can therefore mimic the coalescence of the vortex rings. They related the acoustical emission to the velocity, acceleration and rate of acceleration of the centroid of each ring in order to identify a key mechanism for sound production. The sound predictions obtained by Tang and Ko [13] are of interest for the present study, in particular the presence of high-frequency components already observed by Shariff et al. [12].

Verzicco et al. [14] performed axisymmetric incompressible Navier–Stokes simulations of the merging of two vortex rings. They showed that the contribution of the Reynolds stresses to the acoustical field was largely dominant compared to the contribution of viscous effects. They also found that the high-frequency contribution to their acoustical field was related to the eddy turnover time of the rings.

The progresses in computational aeroacoustics (CAA) allow nowadays a direct numerical simulation (DNS) of the hydrodynamic and acoustical fields at once. Colonius et al. [15] calculated the sound produced by vortex pairing in a plane shear layer using such accurate and non-dispersive CAA code. Mitchell et al. [16], and Zhao et al. [17] performed similar calculations to obtain the sound produced by vortex pairing in an axisymmetrical jet. In a recent study, Inoue [18] predicted the sound produced by the pairing of two vortex rings from DNS data as well. The results indicated that the higher frequencies are related to the orientation of the vortex cores. Yet, the Reynolds numbers of the flows simulated by Inoue [18] are one to three orders of magnitude smaller than the one obtained in these experiments.

Generally speaking, the Reynolds numbers Re that can be achieved by these accurate numerical simulations are still below the range that corresponds to practical engineering applications. Colonius [19] showed that the cost of a CAA calculation is proportional to Re^3M^{-4} for a DNS, and to Re^2M^{-4} for a large eddy simulation. Therefore the Mach number M is usually in the large subsonic range ($\simeq 0.9$) in order to obtain a good accuracy on the calculated sound field, while the Reynolds number is kept low to minimize the computational cost.

Conversely, a low Mach number flow ($M = 0.1$), at a relatively large Reynolds number $Re = O(10^5)$ is considered here. The detailed evolution of the velocity and vorticity fields in the region of the pairing vortex rings has been obtained by means of particle image velocimetry measurements. Results obtained using a large field of view are reported here. Measurements performed with a closer field of view, centred on the core of the pairing rings during their interaction, are described by Schram [20]. It is believed these data are of interest for numerical modelling purposes.

A so-called conservative formulation of the vortex sound theory for axisymmetrical flow is used to predict the sound emission from the PIV data. This formulation was developed in a previous paper [9]. It was shown to be less sensitive to errors in the flow data than the original formulations due to Powell [21] and Möhring [8] from which it is derived. This formulation was applied with

some success to experimental measurements of vortex pairing in a circular air jet with outlet velocity equal to 5.0 m/s. It was shown [10] that the sound prediction agreed both qualitatively and quantitatively with predictions obtained applying Möhring's analogy to a simplified theoretical modelling and a numerical simulation of the same flow. But it was naturally impossible to actually measure the weak sound radiation of such a low speed jet. The present paper concerns the application of the same methodology to a vortex pairing occurring in a circular air jet with outlet velocity equal to 34.2 m/s, and the comparison of the sound prediction with measurements of the sound actually produced by the jet.

This paper is organized as follows: the bases of Vortex Sound Theory, its underlying assumptions and the derivation of the authors' conservative formulation will be briefly recalled. The jet facility and the experimental measurements of the flow field are then described. The post-processing of the particle image velocimetry data and their implementation into the acoustical analogy have been the subject of another paper [10], so that only the main steps will be reviewed here. The acoustical spectrum of vortex pairing will then be predicted, and compared with acoustical measurements.

2. Vortex sound theory, and conservative formulation for axisymmetrical flow

Vortex Sound Theory was developed by Powell [21] for low Mach number flows in free-field conditions. Howe [22] proposed a generalization to wall-bounded flows and arbitrary Mach numbers. For low Mach number, homentropic flows, and in absence of external forces or source of mass, Powell [21] obtained the integral solution for the far-field perturbation:

$$p'(\mathbf{x},t) = -\frac{\rho_0}{4\pi c_0^2|\mathbf{x}|^3}\frac{\partial^2}{\partial t^2}\int\int\int_V (\mathbf{x}\cdot\mathbf{y})\,\mathbf{x}\cdot(\boldsymbol{\omega}\times\mathbf{v})\,\mathrm{d}^3\mathbf{y}, \tag{1}$$

where p' is the acoustical pressure perturbation, $\mathbf{x}$ is the coordinate of the listener, $\mathbf{y}$ is the integration coordinate over the source region, t is time, $\mathbf{v}$ is the velocity and $\boldsymbol{\omega} = \nabla\times\mathbf{v}$ is the vorticity, ρ_0 and c_0 are the density and speed of sound in the propagation region, and all the integrands have to be evaluated at the retarded time $t - |\mathbf{x}|/c_0$.

Imposing one more time the conservation of kinetic energy, Möhring [8] showed that the acoustical source term can be expressed as a function of the vorticity alone:

$$p'(\mathbf{x},t) = \frac{\rho_0}{12\pi c_0^2|\mathbf{x}|^3}\frac{\partial^3}{\partial t^3}\int\int\int_V (\mathbf{x}\cdot\mathbf{y})\,\mathbf{x}\cdot(\mathbf{y}\times\boldsymbol{\omega})\,\mathrm{d}^3\mathbf{y} \tag{2}$$

in which the velocity does not appear anymore.

The same conservation laws have been simply reiterated to obtain Lighthill's quadrupole for homentropic free compact turbulent flows, Powell's solution to the same problem, and finally Möhring's formulation. Although formally equivalent, these analogies do not provide the same robustness when applied to a flow model that does not respect the conservation laws strictly. It has been shown in a previous paper [9] how reiterating conservation laws can be beneficial to the robustness of the sound prediction. On these grounds, a so-called conservative formulation of Vortex Sound Theory has been derived for homentropic, low Mach number axisymmetrical free

flows:

$$p'(\mathbf{x},t)=\frac{\rho_0}{4c_0^2|\mathbf{x}|}\frac{\mathrm{d}^2Q'}{\mathrm{d}t^2}\left(\cos^2\theta-\tfrac{1}{3}\right) \tag{3}$$

with

$$Q'=\int\int_S 3\omega v r\,(z-z_0)\,\mathrm{d}r\,\mathrm{d}z, \tag{4}$$

where (r,z) are the radial and axial coordinates of the fluid elements of radial velocity v and azimuthal vorticity ω, θ is the listener polar angle from the jet axis, and z_0 is the axial coordinate of the centre of gravity of the vortex system defined by Lamb [23] as

$$z_0=\frac{\int\int_S \omega r^2 z\,\mathrm{d}r\,\mathrm{d}z}{\int\int_S \omega r^2\,\mathrm{d}r\,\mathrm{d}z}. \tag{5}$$

3. Experimental characterization of vortex pairing

The present approach makes use of the particle image velocimetry measurement technique. The methodology that has been followed to obtain the PIV data and the post-processing that gives a sound prediction has been described in another paper [10] for the case $U_0=5\,\mathrm{m/s}$, and further details are discussed by Schram [20]. The main lines are summarized in what follows.

3.1. Experimental facility

The experimental facility is sketched in Fig. 1. The nozzle has an outlet diameter $D=0.041\,\mathrm{m}$, and is operated at an outlet velocity $U_0=34.2\,\mathrm{m/s}$. The boundary layer at the nozzle outlet is laminar. The jet discharges in a 4 m (length) × 3 m (width) × 4 m (height) semi-anechoic room, at 0.92 m above the floor. The inner diameter of the cylindrical section upstream of the nozzle contraction is 0.3 m. The cut-off frequency above which non-planar waves propagate in this section is $f_{\text{cut-off}}=0.67\,\mathrm{kHz}$. The cut-off frequency calculated for the section at the end of the contraction, with a diameter of 0.041 m, is $f_{\text{cut-off}}=4.9\,\mathrm{kHz}$.

A stable vortex pairing was obtained using a single frequency acoustical excitation of the shear layer instability. The excitation is provided by a loudspeaker located in the settling chamber (see Fig. 1). Fig. 2 shows the acoustical signal measured using a microphone (Bruel&Kjaer, $\frac{1}{2}$ in) and a spectrum analyzer (Hewlett-Packard, model 35660A) at the nozzle outlet when a white noise signal generated by the same spectrum analyzer is applied to the loudspeaker. A series of resonance peaks below the pipe cut-off frequency $f_{\text{cut-off}}=0.67\,\mathrm{kHz}$ can be observed. Those correspond to the longitudinal resonant modes of the pipe. For the jet outlet velocity $U_0=34.2\,\mathrm{m/s}$ considered here, an excitation frequency $f_e=2.5\,\mathrm{kHz}$ has been chosen on the basis of flow visualizations showing a very stable periodic pairing for these conditions [20]. This frequency is still low compared to the nozzle exit cut-off frequency $f_{\text{cut-off}}=4.9\,\mathrm{kHz}$. The nozzle exit can be approximated by a straight pipe segment with a length of the order of one diameter which imposes a significant reduction of non-planar modes at the excitation frequency $f_e=2.5\,\mathrm{kHz}$.

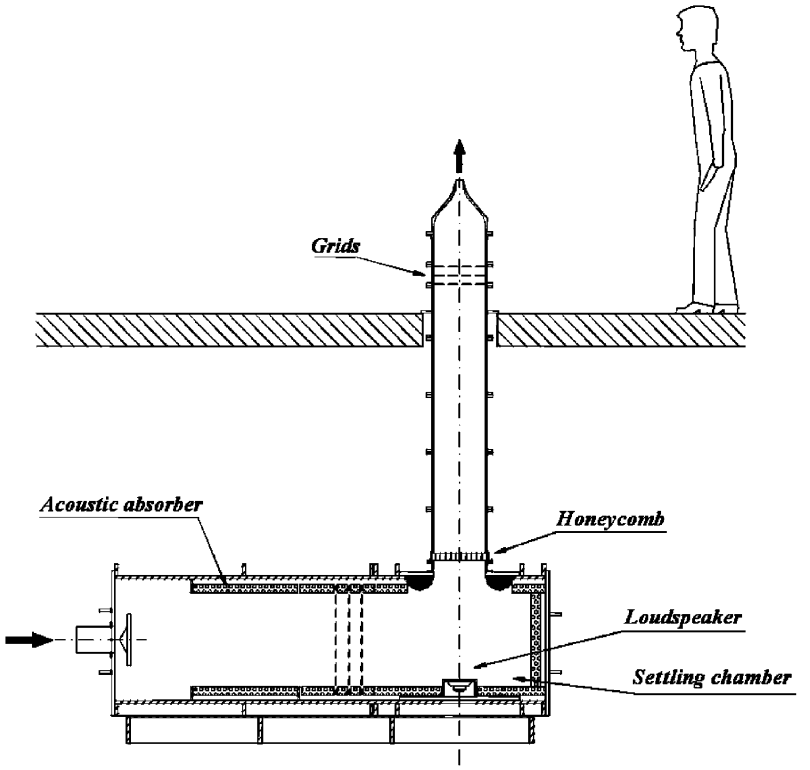

Fig. 1. Experimental facility.

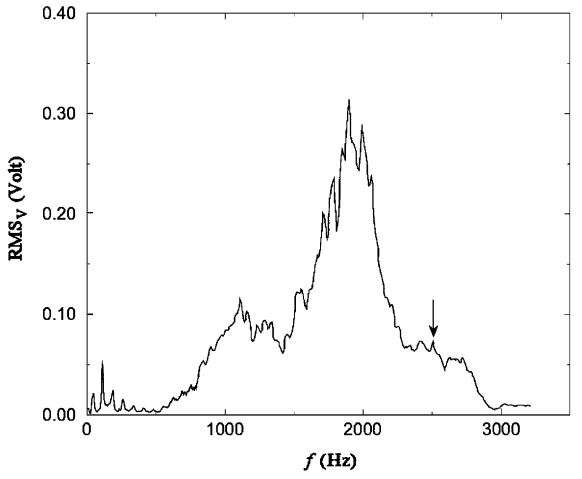

Fig. 2. Spectrum of the acoustical perturbations at the nozzle outlet plane when white noise excitation is applied at the loudspeaker. The arrow indicates the frequency chosen to promote a stable vortex pairing.

In this case the shear layer mode of pairing [24] is promoted by the excitation. The Strouhal number for this mode scales on the jet initial shear layer momentum thickness θ_m, was measured at an axial location $z = D/4$ using hot wire anemometry data, $z = 0$ corresponding to the nozzle outlet plane. The excitation frequency $f_e = 2.5\,\text{kHz}$ yields a Strouhal number $Sr_\theta = f_e\,\theta_m/U_0 = 0.013$, which is in good agreement with the value of 0.012 indicated by Zaman and Hussain [24] for the shear layer pairing mode. This mode was shown by Bridges and Hussain [7] to contribute to a large extent to the acoustical field of unexcited laminar jets. The excitation level is characterized using hot wire anemometry to obtain the acoustical velocity perturbation in the nozzle outlet plane. The excitation amplitude is $u'_e/U_0 = 0.16\%$, where u'_e is the rms value of the velocity oscillation.

3.2. Experimental method

The data has been obtained using stroboscopic PIV [25]. Using the same synchronization technique, but injecting smoke in the boundary layer of the nozzle instead of PIV seeding, yields pseudo-time resolved flow visualizations as illustrated in Fig. 3. The figures are sequenced according to the phase φ defined with respect to the acoustical excitation signal. The pairing period is therefore 4π. The phase $\varphi = 0\,\text{rad}$ is arbitrarily set to correspond to the instant at which the leading and trailing rings, indicated by L and T in Fig. 3, are coplanar. This is known to correspond to the peak acoustical emission [11]. The vortex ring resulting from the merging of the leading and trailing rings is indicated by M in Fig. 3.

The PIV system is extensively described by Schram [20]. Seeding particles (mean diameter 1 μm) are illuminated on a meridian plane of the jet flow using a double-pulsed Nd:YAG laser. Their image is captured by a 12-bit PCO SensiCam® CCD camera with a $1280 \times 1024\,\text{px}^2$ non-interlaced sensor chipset. The pairs of particle images were processed using a PIV software developed at the von Karman Institute for Fluid Dynamics, called WIDIM (WIndow Distortion Iterative Multigrid [26]).

The processing parameters are summarized in Table 1. A vector is validated when the amplitude of the correlation peak is at least 50% larger than the amplitude of the second highest peak.

A sample snapshot shown in Fig. 4 illustrates the field of view of the PIV measurements and their spatial resolution. The x-axis of the PIV measurements is aligned with the jet axis. The spatial discretization $\Delta x = \Delta y$ of the cores of the vortex rings is about $\sigma_c/4$, where σ_c is the radius of the vortex cores before merging.

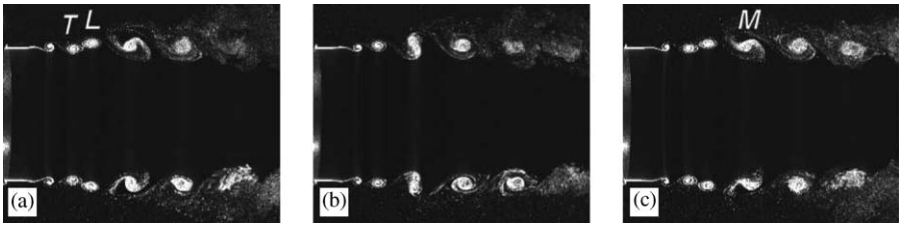

Fig. 3. Smoke visualization of vortex pairing. (a) $\varphi = -5.7\,\text{rad}$, (b) $\varphi = 0\,\text{rad}$, (c) $\varphi = 6.8\,\text{rad}$.

Table 1
Parameters of the PIV interrogation algorithm

Initial window size	$20 \times 20\,\mathrm{px}^2$
Number of refinement steps	1
Final window size W_s	$10 \times 10\,\mathrm{px}^2$
Window overlap	50%
Spatial resolution $\Delta x = \Delta y$	$0.33\,\mathrm{mm} \simeq D/125 \simeq \sigma_c/4$
Validation rate	96%

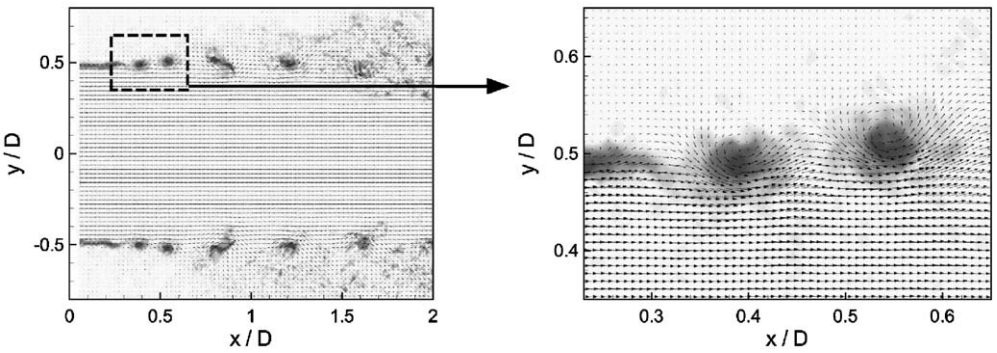

Fig. 4. Field of view of the PIV measurements, and detail of the velocity and vorticity fields sampling across the vortex cores before merging. For readability, every third vector is shown in each direction in the large field of view.

The measurement uncertainty has been evaluated by Schram [20]. The uncertainty on the velocity in the worst case, i.e. in the core of the vortices where the gradient is the largest, is below 2%. The vorticity ω is calculated using a third-order accurate Richardson's scheme, giving a maximum uncertainty below 8%.

4. Prediction of vortex pairing sound

The task is to calculate the pressure perturbation according to Eq. (3). The source term (4) is obtained from the PIV data. In this work it is intended to compare the predicted and measured sound pressure levels at one single point, the directivity of the pairing being left to a further exhaustive study. The polar angle θ is equal to 90°. This choice is motivated by the results of Bridges and Hussain [27]. They showed that the evolution of the pairing vortices near the nozzle outlet can generate a dipolar contribution at least as strong as the quadrupole when the pairing occurs.

However, the directivity of the induced dipole is $(1 - \cos\theta)$ as long as the vorticity evolution remains axisymmetric close to the nozzle [28]. It was therefore decided to place the microphone at 90° from the jet axis to avoid contamination of the quadrupole with a possible dipole.

4.1. Implementation of the PIV data

The major issue to calculate the integral source term Q' defined by Eq. (4) is the definition of the integration domain. The method is based on a vortex detection algorithm developed in a previous work [20,25]. This allows automatic processing of the PIV series and definition of an integration window centred on the pairing vortices as they evolve in the field of view.

Fig. 5 shows the axial position of the vortex rings cores during their interaction, obtained using the vortex detection algorithm. A linear fit of these data gives the trajectory of the integration window, which follows the two vortices at a constant speed $U_w = 0.57U_0$. The axial extent of the integration window is $\Delta x = 0.3D$. This length includes the significant vorticity levels of the pairing vortices alone (see Fig. 6).

The expression for Q' in Eq. (3) is expressed assuming axisymmetry around the jet axis, i.e. the x-axis in the PIV system of coordinates. The integration in Eq. (3) is therefore performed

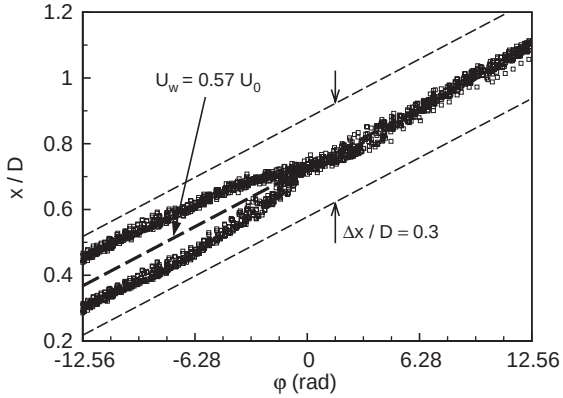

Fig. 5. Axial position of the vortex cores and definition of the integration domain.

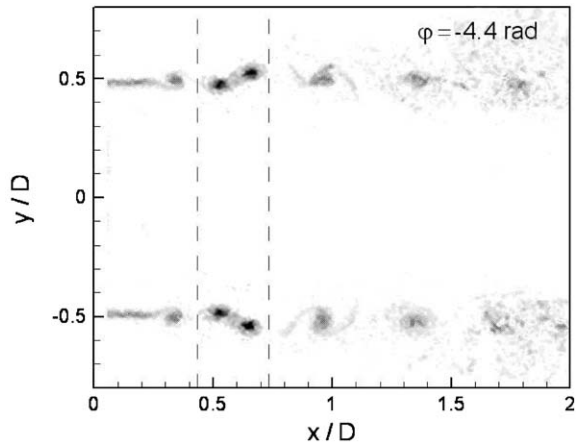

Fig. 6. Integration window.

separately over each half-plane $y>0$ and $y<0$, and both results are averaged together. This allows one to filter out asymmetric vortex motion [20].

Fig. 7 shows the integral term Q', each symbol representing the result of the integration of one PIV field. Ninety series of 32 PIV fields have been processed. The two vortex rings have been tracked from $\varphi = -4\pi \simeq -12.56$ rad when they have both detached from the shear layer, until $\varphi = 6\pi \simeq 25.12$ rad when the merged ring exits the field of view. An important scatter in the data can be seen for $\varphi > 4\pi \simeq 12.56$ rad. It has been observed that this is due to growing asymmetric instabilities and occasionally breakdown of the merged ring.

To calculate the second time derivative of the source term Q' (see Eq. (3)), the data points over a moving interval have been fitted by a fourth-order polynomial. The line in Fig. 7 is obtained by evaluation of the polynomial at the centre of each interval. Fig. 8 shows the second derivative of the polynomials evaluated at the centre of each moving window. The length of the fitting interval

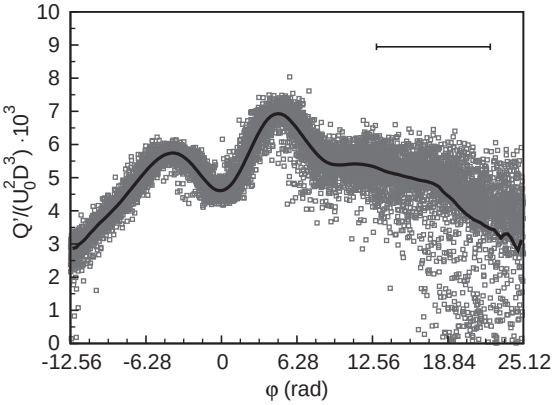

Fig. 7. Integral source term Q'. □ : integral (4) calculated for each PIV field ; — : fourth-order polynomial fit.

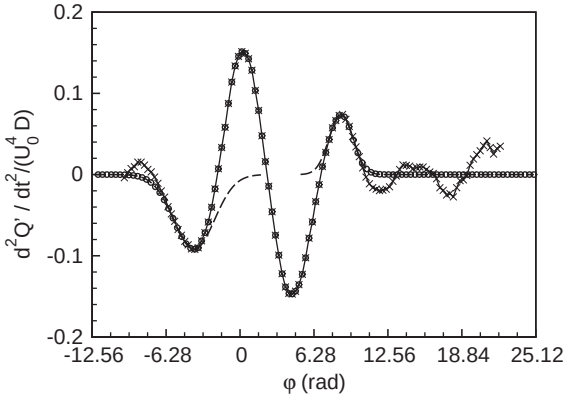

Fig. 8. Acoustical source term d^2Q'/dt^2. –×– : original source term ; – – : Gaussian fit functions ; ○ : corrected source term.

is represented in the top-right corner of Fig. 7. Shorter windows were used to fit the data at the smaller and larger abscissa.

The resulting acoustical source term shown in Fig. 8 exhibits some interesting features. First, compared to the relatively localized acoustical pulse generated by the pairing at the lower jet velocity previously investigated by Schram et al. [10] ($U_0 = 5\,\mathrm{m/s}$), the sound produced at 34.2 m/s is seen to contain higher frequencies. Secondly, the pressure fluctuation has a duration exceeding the pairing period. This is due to the fact that the time needed to achieve a vortex merging lasts longer than two excitation periods. In order to predict the sound spectrum actually produced by the periodic vortex pairing in such case, one has therefore to superimpose the time traces corresponding to several pairings, shifted with respect to each other by a phase of 4π rad. This assumes implicitly that the variation of the time of propagation between the pairing vortices and the listener, over the region in which pairing occurs, is negligible compared to the acoustic period. However, this hypothesis is not more restrictive than assuming a compact source, since the spatial extent of the region over which pairing occurs is smaller than a nozzle diameter.

In order to avoid steps generating spurious high frequencies, one has to smoothly truncate the signal at its extremities before phase shifting and addition. Fig. 8 shows how this was performed by fitting the beginning and end of the acoustical source term using Gaussian functions.

4.2. Predicted pressure time trace and spectrum

To minimize edge effects in the subsequent Fourier transform, one thousand shifted acoustical source terms signals have been summed together. The acoustical pressure (3) has been calculated using $|\mathbf{x}| = 0.9\,\mathrm{m}$ and $\theta = 90^\circ$, which is the position of the microphone. Fig. 9 shows a portion of this pressure signal. The time axis has been calculated using $t = \varphi/(2\pi f_{\mathrm{exc}})$ where the excitation frequency $f_{\mathrm{exc}} = 2.5\,\mathrm{kHz}$. The spectrum of the sound pressure level, based on a reference pressure of 20 μPa, is shown in Fig. 10. It can be seen that higher harmonics up to 10 kHz are generated in addition to the pairing (i.e. replication) frequency of 1.25 kHz. A large contribution after the pairing fundamental corresponds to the first harmonic at 2.5 kHz. Harmonics at frequencies larger than 5 kHz are much less significant.

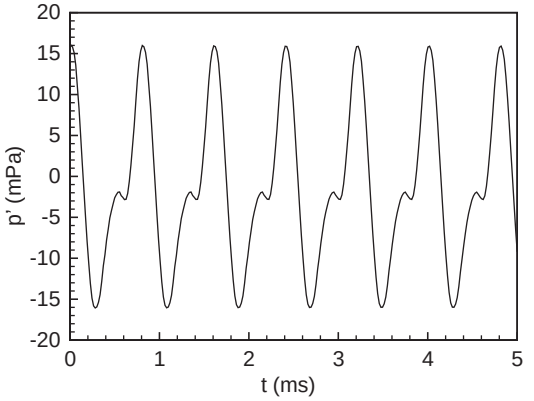

Fig. 9. Acoustical pressure perturbation ($|\mathbf{x}| = 0.9\,\mathrm{m}$, $\theta = 90^\circ$).

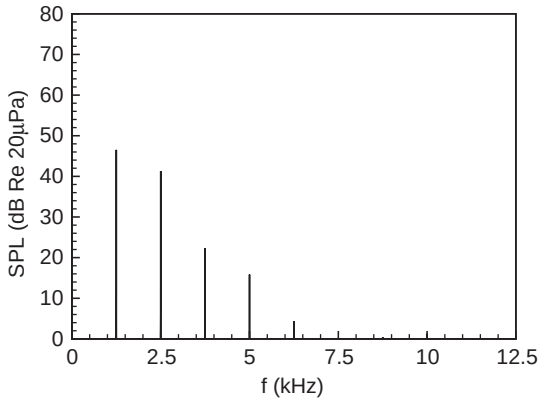

Fig. 10. Sound pressure level spectrum generated by vortex pairing ($|\mathbf{x}| = 0.9\,\mathrm{m}$, $\theta = 90^\circ$).

It is interesting to note that the first harmonic at 2.5 kHz is a significant contribution to the spectrum. It corresponds approximately to the eddy turnover time of each vortex. This value has been evaluated on the basis of detailed PIV measurements focused on the pairing vortices before pairing. The measured vorticity field has been least-square fitted by Oseen vortex models, to yield the circulation, core size and turnover time of the vortices [20]. A turnover time of 0.42 ms has been obtained, which gives a nutation frequency equal to 2.375 kHz. This result is consistent with previous observations made by several authors [12–14] about the frequencies emitted by vortex merging.

5. Acoustical measurements

The acoustical measurements were performed in the semi-anechoic room recently built at the von Kármán Institute for Fluid Dynamics. The cut-off frequency of the room is 350 Hz.

The acoustical measurements were performed using $\frac{1}{2}$ inch B&K microphones (types 4133 and 2669) and B&K charge amplifiers (types 5935 and 5935L). The signal from the charge amplifiers has been high-pass filtered at 100 Hz and low-pass filtered at 12 kHz. A sampling frequency of 25 kHz has been used.

For all the acoustical measurements described here, the microphone membrane is located in the nozzle outlet plane at a distance of 0.9 m from the jet axis. The microphone output has been calibrated using a pistonphone. Ten series of 10 922 points were acquired. The spectrum for each series was calculated applying Welch's averaging method, using intervals of 512 points overlapping over 256 points. The resulting frequency resolution is 48.8 Hz.

A difficulty in the present measurements was the low sound pressure level emitted by the jet at $M = 0.1$. For this reason, the measurements were conducted during night to avoid any external pollution. The background noise is represented in Fig. 11. It can be seen that the ambient sound pressure level is below 10 dB for frequencies above 1 kHz.

The jet outlet velocity for the rest of the measurements is $U_0 = 34.2\,\mathrm{m/s}$, with a deviation over time of less than 1%.

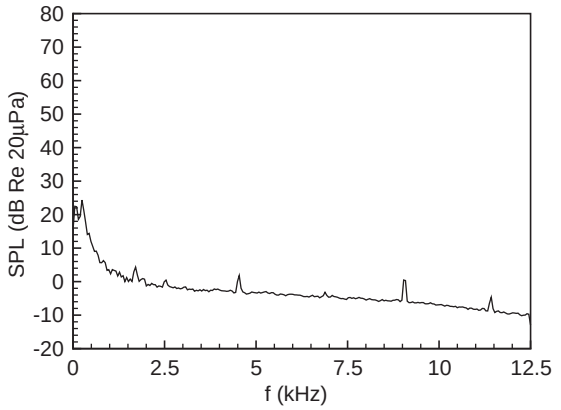

Fig. 11. Background noise in the acoustic room.

5.1. Broadband suppression under acoustical forcing, and intermittent double pairing

The sound produced by the acoustical excitation has been measured without flow. The spectrum in Fig. 12 shows that the noise provided by the loudspeaker at 2.5 kHz has a quite pure harmonic content, the first higher harmonic at 5 kHz being 52 dB smaller than the fundamental. This figure shows also that the loudspeaker signal does not contain any subharmonic component, which will be important for the interpretation of the sound spectra in presence of the flow.

Fig. 13 shows an ensemble-averaged spectrum calculated from acoustical measurements performed with the jet at 34.2 m/s, at 0.9 m from the nozzle outlet and at 90° from the jet axis, with and without acoustical excitation. Ten series have been used for the averaging. The excitation causes a concentration of the acoustical spectrum in discrete frequencies, while the broadband noise is seen to decrease significantly for frequencies between the discrete peaks. This broadband suppression is consistent with observations made by several authors in similar conditions [29,30] and others discussed by Crighton [31]. Please note that for the present forcing conditions, the decrease of broadband noise is largely compensated by the tonal components, the overall sound pressure level (OASPL) being 53.3 dB without excitation and 74.3 dB with excitation.

Considering the discrete frequencies that are amplified due to the excitation, the largest component after the excitation at 2.5 kHz has a frequency equal to 1.25 kHz. This component can be univocally attributed to some vortex pairing, being given the absence of subharmonic in the loudspeaker signal. The second largest component has a frequency equal to 625 kHz, which following the same argument can be attributed to a subsequent pairing of the merged rings resulting from the first pairing. The higher harmonics of each pairing and of the excitation can then be traced along the spectrum in Fig. 13, as indicated by the "1P", "2P" and "EXC" labels.

The analysis of individual spectra revealed that the second pairing occurs intermittently. An individual sound spectrum obtained without second pairing occurrence is shown in Fig. 14. Observing that the amplitudes of the peaks at 1.25, 3.75 and 6.25 kHz from Figs. 13 (excited case) and 14 have the same amplitude, it is concluded that the contribution of the second pairing to the frequencies concerned by the first one is negligible.

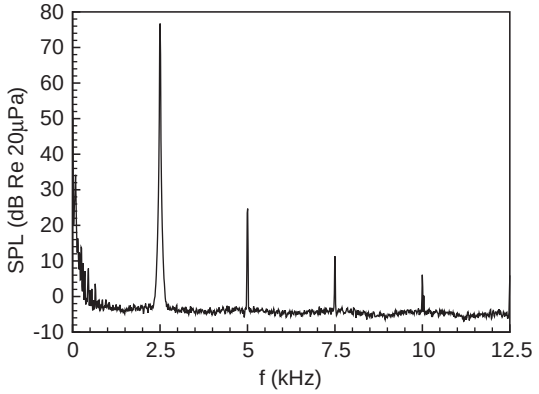

Fig. 12. Sound spectrum of the excitation alone at 2.5 kHz (no flow), measured at a distance of 0.9 m from the nozzle outlet and 60° from the jet axis.

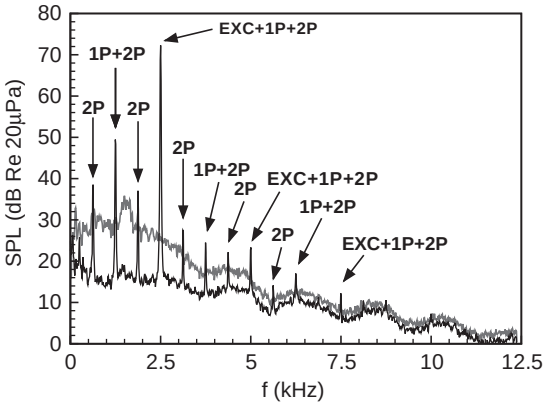

Fig. 13. Broadband noise suppression, average spectrum over 10 realizations. Thick line: unexcited jet ; thin line: excited jet. The labels "1P", "2P" and "EXC" indicate when the first pairing, second pairing and excitation contribute to each frequency peak.

5.2. Comparison with theoretical prediction

Fig. 15 shows the predicted spectrum (symbols) superimposed to the single pairing spectrum of Fig. 14 (line). A good quantitative agreement is observed between the predicted amplitude and the measured one for the frequencies not contaminated by the acoustical excitation: 1.25 and 3.75 kHz. The predictions at 6.25 kHz and higher frequencies are below the measured background noise level. The measured spectrum nevertheless shows significant peaks above the background noise at frequencies that can be attributed to the pairing: 6.25 and 8.75 kHz. These peaks are largely underestimated in the prediction, presumably due to the smoothing process involved in the polynomial fit shown in Fig. 7. It is likely that individual vortex pairings produce more sound

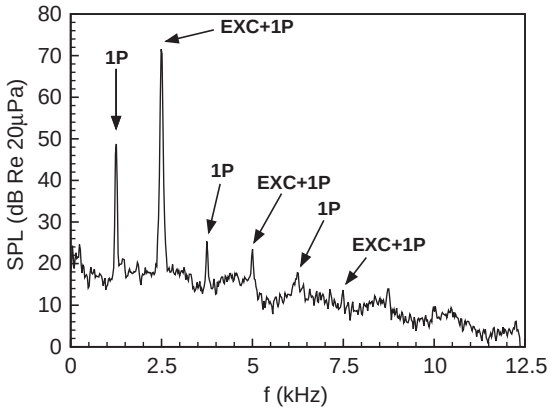

Fig. 14. Spectrum calculated using a single time series, exhibiting the absence of double pairing.

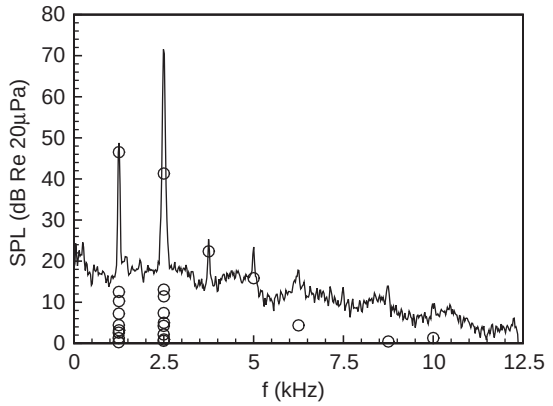

Fig. 15. Comparison of predicted (symbols) and measured (line) sound pressure level spectrum, at a distance of 0.9 m from the nozzle outlet and 90° from the jet axis.

than the ensemble-averaged pairing obtained from the measurements, especially at high-frequency harmonics.

Such agreement between the prediction and the measurements is nevertheless remarkable for the 1.25 and 3.75 kHz components. The frequency of 1.25 kHz is the one of leapfrogging of the trailing ring inside the leading one. The predicted amplitude at the frequency 2.5 kHz is associated to the vortex core nutation. It is naturally regrettable that the acoustical excitation overwhelms this frequency component. Further study of the directivity of this component might give a better insight, on the basis that the acoustical excitation should produce a monopole—neglecting sound diffraction at the nozzle outlet for the low frequencies considered here, while the pairing should contribute as a quadrupole with a $(\cos^2\theta - \frac{1}{3})$ directivity. A possible discrepancy with this theoretical directivity could have a super-directive cause as described by Crighton and Huerre [32]. But this issue is beyond the scope of the present paper, and is left to further investigations.

6. Conclusions

The present work is a follow-up of previous contributions. A so-called conservative formulation (3) of the vortex sound theory was derived by Schram et al. [9] from the original versions (1) and (2) of Powell [21] and Möhring [8]. This form was first applied to perturbed vortex leapfrogging models to yield sound prediction in agreement with the literature. In a second paper, the vortex pairing in a low velocity jet (5.0 m/s) was considered and the sound prediction obtained was shown to agree with numerical simulation of the sound emitted by the same flow [10]. The authors' now consider a jet flow at a higher velocity for which the sound field actually produced by vortex pairing is measurable.

In order to compare the sound prediction with the measurements, a sound spectrum has been calculated from the acoustical time trace obtained from the PIV measurements. The spectrum emitted by the pairing is made of the pairing frequency and higher harmonics. The most significant harmonic is the first one, at a frequency close to the vortex core nutation frequency, which agrees with existing literature. Harmonics above the third one (at 5 kHz) are negligible.

Sound spectra obtained with and without acoustical forcing of the jet have shown a broadband cancellation in agreement with previous observations. The OASPL increases however significantly with the present forcing level.

The discrete frequency components of the measured spectrum have been attributed to the acoustical excitation, the first vortex pairing and an intermittent second pairing. The intermittent second pairing does not seem to contribute significantly to the frequency components associated to the first pairing.

A good agreement is found between the sound prediction and the measured sound spectrum at frequencies not contaminated by the acoustical excitation. This is to the authors' knowledge the first quantitative prediction of the sound produced by a vortex interaction described by experimental data. This result could be obtained thanks to the robustness of the conservative formulation (3).

Acknowledgements

The present research was funded by, and conducted at the von Kármán Institute for Fluid Dynamics. The authors thank Ann Dowling and Tim Colonius for fruitful discussions.

References

[1] M.J. Lighthill, On sound generated aerodynamically. Part I. General theory, *Proceedings of the Royal Society of London* A 211 (1952) 564–587.

[2] M.J. Lighthill, On sound generated aerodynamically. Part II. Turbulence as a source of sound, *Proceedings of the Royal Society of London* A 222 (1954) 1–32.

[3] J.E. Bridges, Application of Coherent Structure and Vortex Sound Theories to Jet Noise, Ph.D. Thesis, University of Houston, 1990.

[4] J.E. Bridges, A.K.M.F. Hussain, Direct evaluation of aeroacoustic theory in a jet, *Journal of Fluid Mechanics* 240 (1992) 469–501.

[5] A. Powell, Three-sound-pressure theorem, and its application, in aerodynamically sound, *Journal of the Acoustical Society of America* 34 (7) (1962) 902–906.
[6] K.W. Ryu, D.J. Lee, Sound radiation from elliptic vortex rings: evolution and interaction, *Journal of Sound and Vibration* 200 (3) (1997) 281–301.
[7] J.E. Bridges, A.K.M.F. Hussain, Roles of initial conditions and vortex pairing in jet noise, *Journal of Sound and Vibration* 117 (2) (1987) 289–311.
[8] W. Möhring, On vortex sound at low Mach number, *Journal of Fluid Mechanics* 85 (1978) 85–691.
[9] C. Schram, A. Hirschberg, Application of Vortex Sound Theory to vortex-pairing noise: sensitivity to errors in flow data, *Journal of Sound and Vibration* 266 (2003) 1079–1098.
[10] C. Schram, A. Hirschberg, R. Verzicco, Sound produced by vortex pairing: prediction based on particle image velocimetry, *AIAA Journal*, in press.
[11] T. Kambe, T. Minota, Sound radiation from vortex systems, *Journal of Sound and Vibration* 74 (1) (1981) 61–72.
[12] K. Shariff, A. Leonard, N.J. Zabusky, J.H. Ferziger, Acoustics and dynamics of coaxial interacting vortex rings, *Fluid Dynamics Research* 3 (1988) 337–343.
[13] S.K. Tang, N.W.M. Ko, On sound generated from the interaction of two inviscid coaxial vortex rings moving in the same direction, *Journal of Sound and Vibration* 187 (2) (1995) 287–310.
[14] R. Verzicco, A. Iafrati, G. Riccardi, M. Fatica, Analysis of the sound generated by the pairing of two axisymmetric co-rotating vortex rings, *Journal of Sound and Vibration* 200 (3) (1997) 347–358.
[15] T. Colonius, S.K. Lele, P. Moin, Sound generation in a mixing layer, *Journal of Fluid Mechanics* 330 (1997) 375–409.
[16] B.E. Mitchell, S.K. Lele, P. Moin, Direct computation of the sound generated by vortex pairing in an axisymmetric jet, *Journal of Fluid Mechanics* 383 (1999) 113–142.
[17] W. Zhao, S.H. Frankel, L. Mongeau, Effects of spatial filtering on sound radiation from a subsonic axisymmetric jet, *AIAA Journal* 38 (11) (2000) 2032–2039.
[18] O. Inoue, Sound generation by the leapfrogging between two coaxial vortex rings, *Physics of Fluids* 14 (9) (2002) 3361–3364.
[19] T. Colonius, Lectures on Computational Aeroacoustics, Aeroacoustics and Active Noise Control, von Karman Institute LS 1997-07, 1997.
[20] C. Schram, Aeroacoustics of Subsonic Jets: Prediction of the Sound Produced by Vortex Pairing Based on Particle Image Velocimetry, Ph.D. Thesis, Technische Universiteit Eindhoven, 2003.
[21] A. Powell, Theory of vortex sound, *Journal of the Acoustical Society of America* 36 (1) (1964) 177–195.
[22] M.S. Howe, Contribution to the theory of aerodynamic sound, with application to excess jet noise and the theory of the flute, *Journal of Fluid Mechanics* 71 (1975) 625–673.
[23] H. Lamb, *Hydrodynamics*, 6th ed., Cambridge University Press, London, 1932.
[24] K.B.M. Zaman, A.K.M.F. Hussain, Vortex pairing in a circular jet under controlled excitation. Part 1. General jet response, *Journal of Fluid Mechanics* 101 (4) (1980) 449–491.
[25] C. Schram, M.L. Riethmuller, Measurement of vortex ring characteristics during pairing in a forced subsonic air jet, *Experiments in Fluids* 33 (2002) 879–888.
[26] F. Scarano, M.L. Riethmuller, Advances in iterative multigrid PIV image processing, *Experiments in Fluids* 29 (2000) S051–S060.
[27] J.E. Bridges, A.K.M.F. Hussain, Effects of nozzle body on jet noise, *Journal of Sound and Vibration* 188 (3) (1992) 407–418.
[28] M.S. Howe, *Acoustics of Fluid–Structure Interactions, Cambridge Monographs on Mechanics*, Cambridge University Press, Cambridge, 1998.
[29] S.C. Crow, F.H. Champagne, Orderly structure in jet turbulence, *Journal of Fluid Mechanics* 48 (3) (1971) 547–591.
[30] J. Laufer, T.C. Yen, Noise generation by a low-Mach-number jet, *Journal of Fluid Mechanics* 134 (1983) 1–31.
[31] D.G. Crighton, Acoustics as a branch of fluid mechanics, *Journal of Fluid Mechanics* 106 (1981) 261–298.
[32] D.G. Crighton, P. Huerre, Shear-layer pressure fluctuations and superdirective acoustic sources, *Journal of Fluid Mechanics* 220 (1990) 355–368.